

**PREPARATION AND CHARACTERIZATION OF CARBON DOPED TiO₂
USING HUMIC ACID AND ITS MODIFIED DERIVATIVE AS CARBON
PRECURSORS FOR ENHANCED PHOTOCATALYTIC ACTIVITIES**

by

ISMARIZA BINTI ISMAIL

**Thesis submitted in fulfillment of the requirements
for the degree of
Master of Science**

JAN 2011

ACKNOWLEDGEMENTS

I would like to express my eternal gratitude to my supervisor, Prof Mohd. Asri Mohd. Nawi for his proficient supervision throughout my candidature. His guidance and constructive criticism always gave me confidence to carry on with the work whenever there were any obstacles. The invaluable encouragement would never be disregarded. Only God could pay all of his good deeds.

I am grateful to all the staff of the School of Chemical Sciences who never failed to entertain me even though they are engaged with their critical duties. Thank you for the cooperation and assistance provided. Not forgetting, heartfelt thanks to all my fellow graduate students who shared a lot with me during those precious times.

My special dedication goes to my husband and family for their never ending moral support and patience. I wish to acknowledge their inspiration during the hard time that I had in completing the studies.

I wish to thanks USM for the financial support awarded to me under USM fellowship scheme throughout my two years of research. Finally, a big appreciation to everyone that contributed one way or another to the wonderful time I had at School of Chemical Sciences.

TABLE OF CONTENTS

Acknowledgement	ii
Table of Contents	iii
List of Tables	ix
List of Figures	x
List of Abbreviations	xviii
Abstrak	xix
Abstract	xxi

CHAPTER 1: INTRODUCTION AND LITERATURE REVIEW

1.1	General	1
1.2	Semiconductor Photocatalyst	2
1.3	Basic Principle of Photocatalysis	4
1.4	Titanium Dioxide versus Existing Photocatalyst	6
1.5	General Mechanism of TiO ₂ - assisted Photocatalytic Degradation of Pollutants	11
1.6	Improving TiO ₂ Photocatalytic Activity	13
	1.6.1 Modification with metals	14
	1.6.2 Modification with non-metals	15
	1.6.3 Modification with CdS: Composite semiconductors	19
	1.6.4 Dye sensitized titanium dioxide photocatalyst	20
1.7	Potential Natural Products for TiO ₂ Sensitizers and Carbon Precursors	22
	1.7.1 Humic acids	22

1.7.2	Peat coagulant	23
1.8	Reactive Red 4 Dye	24
1.9	Problems Statement	25
1.10	Research Outline and Objectives	26
CHAPTER 2: METHODOLOGY		
2.1	Reagents and Chemicals	28
2.2	Photoreactor and Light Source	29
2.3	Instruments and Equipments	30
2.4	Preparation of Standard Solutions	31
2.4.1	Preparation of RR4 dye standard solution	31
2.4.2	Preparation of phenol standard solution	32
2.4.3	Preparation of COD reagent for mineralization study of the model pollutant	32
2.5	Modification of TiO ₂ by Carbon Doping	33
2.5.1	Preparation of the carbon precursor	33
2.5.1.1	Preparation of humic acids stock solution	33
2.5.1.2	Preparation of peat coagulant	33
2.5.2	Preparation of the carbon doped TiO ₂ photocatalyst	34
2.5.2.1	Preparation of humic acid doped TiO ₂ particles (THA)	34
2.5.2.2	Preparation of peat coagulant doped TiO ₂ particles (TPC)	34
2.5.2.3	Preparation of carbon doped TiO ₂ with HA as carbon precursor (CTHA)	35

2.5.2.4	Preparation of carbon doped TiO ₂ with PC as carbon precursor (CTPC)	35
2.6	Optimization Studies on the Preparation of Carbon Doped TiO ₂	36
2.6.1	The effect of doping percentage of the carbon precursor on the photocatalytic efficiency of the photocatalyst	36
2.6.2	The effect of sonication time of the TiO ₂ -precursor mixture solution on the photocatalytic efficiency of the modified photocatalyst	37
2.6.3	The effect of calcination temperature on the photocatalytic efficiency of the modified photocatalyst	37
2.7	Characterization of the Photocatalyst	38
2.7.1	SEM-EDX analysis	38
2.7.2	CHNS analysis	38
2.7.3	UV-Vis diffused reflectance	39
2.7.4	BET surface area analysis	39
2.7.5	FT-IR analysis	39
2.7.6	X-ray diffraction (XRD) analysis	40
2.7.7	Photoluminescence analysis	40
2.8	Decomposition of RR4	40
2.9	Determination of Photocatalytic Activity	41
2.10	Controlled Experiments	42
2.11	The Effect of Operational Parameters on the Photocatalytic Efficiency of the Carbon Doped TiO ₂ in the Degradation of RR4 Dye	43
2.11.1	The effect of initial concentration of RR4 dye solution	43

2.11.2	The effect of the photocatalyst dosage	44
2.11.3	The effect of the aeration flow rate	44
2.11.4	The effect of initial pH values of the RR4 dye solutions	45
2.12	Determination of the pH of the Point of Zero Charge (pH_{zpc}) for the Unmodified and Modified Photocatalysts	45
2.13	Phenol as the Second Model Pollutant	46
2.14	Mineralization Study of RR4	46
2.15	Regeneration of the Photocatalyst	48

CHAPTER 3: RESULTS AND DISCUSSION

3.1	Introduction	49
3.2	Screening Experiments	52
3.2.1	Effect of the dopant dosage on the photocatalytic activity of the doped TiO_2	52
3.2.2	Effect of the sonication time of the TiO_2 -dopant solution mixture on the photocatalytic activity of the doped photocatalyst	61
3.2.3	Effect of thermal treatment temperature on the photocatalytic activity of the doped photocatalyst	62
3.3	Physical Characterization of the Carbon Doped TiO_2	65
3.3.1	Carbon content of carbon doped TiO_2 at different doping percentage and calcination temperatures.	65
3.3.2	SEM-EDX analysis	70
3.3.3	BET surface area analysis	73
3.3.4	UV- visible absorption spectrum	74

3.3.5	X-ray diffraction spectroscopy	78
3.3.6	Photoluminescence spectroscopy	80
3.3.7	FTIR spectroscopy	84
3.4	Photocatalytic Evaluation of the Carbon Doped TiO ₂ Samples	86
3.4.1	Adsorption and direct photolysis	86
3.4.2	The relationship between rate constant, <i>k</i> and carbon content	88
3.4.3	Carbon doped TiO ₂ versus unmodified anatase TiO ₂	91
3.4.4	Photodegradation of RR4 dye by visible light and solar illumination	94
3.5	The Operational Parameters Governing the Photocatalytic Degradation of RR4 Dye by the Carbon Doped TiO ₂ Samples	99
3.5.1	Effect of initial dye concentration on the photocatalytic efficiency of carbon doped TiO ₂	99
3.5.2	Effect of catalyst loading on the photocatalytic efficiency of carbon doped TiO ₂	104
3.5.3	Effect of aeration flow rate on the photocatalytic efficiency of carbon doped TiO ₂	108
3.5.4	Effect of initial pH of the RR4 dye solutions on the photocatalytic efficiency of carbon doped TiO ₂	112
3.6	Photocatalytic Mineralization of RR4 Dye	116
3.7	Phenol as the Second Model Pollutant	121
3.8	Regeneration of the Photocatalyst	126

CHAPTER 4: CONCLUSIONS 128

REFERENCES 132

APPENDICES

Appendix A Seminars, conferences or symposiums participated
during candidature

Appendix B Calculation and preparation

Appendix C Data

LIST OF TABLES

		Page
Table 1.1	Band gap energies of selected semiconductors	7
Table 3.1	CHN analysis for humic acid and peat coagulant.	50
Table 3.2	Characteristics of carbon doped TiO ₂ samples prepared from PC precursor	68
Table 3.3	Characteristics of carbon doped TiO ₂ samples prepared from HA precursor	69
Table 3.4	Average particle size and BET surface area of selected photocatalysts	71
Table 3.5	The bandgap energy of the unmodified TiO ₂ and selected carbon doped TiO ₂ samples	77
Table 3.6	Comparison of the peak ratios of the optimum sample of CTHA and CTPC photocatalysts	82
Table 3.7	First order rate constant of the photocatalysts on the photodegradation of RR4 under different light sources	97

LIST OF FIGURES

		Page
Figure 1.1	Schematic diagram on the general mechanism of TiO ₂ photocatalyst	6
Figure 1.2	Positions of the redox potentials of various metallic couples related to the energy levels of the conduction and valence band of TiO ₂	9
Figure 1.3	Crystal structure of (a) anatase and (b) rutile	10
Figure 1.4	Several mechanism of modified TiO ₂ photocatalysts	13
Figure 1.5	Molecular structure of RR4 dye	25
Figure 2.1	Schematic diagram of the photocatalytic degradation of RR4 dye by unmodified and modified TiO ₂	29
Figure 2.2	Schematic diagram of mineralization study of RR4 dye solution by unmodified and modified TiO ₂	47
Figure 3.1	Model structure of humic acid	49
Figure 3.2	Simplified reaction equation for the preparation of peat coagulant from humic acid and ethylenediamine where R is the chemical backbone of a humic acid structure	50
Figure 3.3	Schematic diagram of the preparation process of carbon doped TiO ₂	52

Figure 3.4	Kinetic curves of RR4 dye photodegradation by THA photocatalysts at different doping percentage. Experimental conditions; dye concentration: 30 ppm, catalyst loading: 1.3 gL ⁻¹ , aeration flow rate: 400 mL min ⁻¹ , initial dye pH: ~6.5, light source: 45 watts compact fluorescent lamp	54
Figure 3.5	Kinetic curves of RR4 dye photodegradation by TPC photocatalysts at different doping percentage. Experimental conditions; dye concentration: 30 ppm, catalyst loading: 1.3 gL ⁻¹ , aeration flow rate: 400 mL min ⁻¹ , initial dye pH: ~6.5, light source: 45 watts compact fluorescent lamp	55
Figure 3.6	The effect of HA doping percentage on the photocatalytic activity of the photocatalysts. Experimental conditions; dye concentration: 30 ppm, catalyst loading: 1.3 gL ⁻¹ , aeration flow rate: 400 mL min ⁻¹ , initial dye pH: ~6.5, light source: 45 watts compact fluorescent lamp	56
Figure 3.7	The effect of PC doping percentage on the photocatalytic activity of the photocatalysts. Experimental conditions; dye concentration: 30 ppm, catalyst loading: 1.3 gL ⁻¹ , aeration flow rate: 400 mL min ⁻¹ , initial dye pH: ~6.5, light source: 45 watts compact fluorescent lamp	56
Figure 3.8	Optical absorption spectra of THA samples at different dosage of HA dopant	57

Figure 3.9	Optical absorption spectra of TPC samples at different dosage of PC dopant	58
Figure 3.10	Plot of visible light absorbance of the photocatalyst at 450 nm versus the doping percentage	60
Figure 3.11	The effect of sonication time of the solution mixture on the photocatalytic activity of the photocatalysts. Experimental conditions; dye concentration: 30 ppm, catalyst loading: 1.3 gL ⁻¹ , aeration flow rate: 400 mL min ⁻¹ , initial dye pH: ~6.5, light source: 45 watts compact fluorescent lamp	62
Figure 3.12	The effect of calcination temperature on the photocatalytic activity of CTHA0.025 photocatalysts. Experimental conditions; dye concentration: 30 ppm, catalyst loading: 1.3 gL ⁻¹ , aeration flow rate: 400 mL min ⁻¹ , initial dye pH: ~6.5, light source: 45 watts compact fluorescent lamp	64
Figure 3.13	The effect of calcination temperature on the photocatalytic activity of CTPC0.20 photocatalysts. Experimental conditions; dye concentration: 30 ppm, catalyst loading: 1.3 gL ⁻¹ , aeration flow rate: 400 mL min ⁻¹ , initial dye pH: ~6.5, light source: 45 watts compact fluorescent lamp	65

Figure 3.14	SEM micrograph of (a) Unmodified TiO ₂ (b) CTPC0.20/620 and (c) CTHA0.025/650 photocatalysts at 50 000x magnification	72
Figure 3.15	EDX analysis of carbon doped TiO ₂ photocatalysts	73
Figure 3.16	Optical absorption spectra of unmodified TiO ₂ and CTHA photocatalysts at different carbon concentration; calcination temperature: 650 °C	75
Figure 3.17	Optical absorption spectra of unmodified TiO ₂ and CTPC photocatalysts at different carbon concentration; calcination temperature: 620 °C	77
Figure 3.18	X-ray diffraction pattern of unmodified TiO ₂ and carbon doped TiO ₂ . (a) Unmodified TiO ₂ ; (b) CTHA0.025/650; (c) CTPC0.20/620; (d) CTHA0.025/700; (e) CTPC0.20/700	79
Figure 3.19	Photoluminescence spectra of CTHA photocatalysts at different carbon concentration; calcination temperature: 650 °C	82
Figure 3.20	Photoluminescence spectra of CTPC photocatalysts at different carbon concentration; calcination temperature: 620 °C	83
Figure 3.21	FTIR spectra. (a) Humic acid and (b) Peat coagulant	85
Figure 3.22	FTIR spectra of the photocatalysts. (a) Unmodified TiO ₂ ; (b) CTHA0.025/650; and	86

(c) CTPC0.20/620

Figure 3.23	Adsorption of RR4 by the unmodified TiO ₂ and carbon doped TiO ₂ samples. Experimental conditions; dye concentration: 30 ppm, catalyst loading: 1.3 gL ⁻¹ , aeration flow rate: 400 mL min ⁻¹ , initial dye pH: ~6.5	88
Figure 3.24	Relation between carbon content and photocatalytic activities of CTPC photocatalysts prepared at various treatment temperatures	90
Figure 3.25	Relation between carbon content and photocatalytic activities of CTHA photocatalysts prepared at 650 °C	91
Figure 3.26	Decomposition of RR4 dye over unmodified TiO ₂ and carbon doped TiO ₂ photocatalysts. Experimental conditions; dye concentration: 30 ppm, catalyst loading: 1.3 gL ⁻¹ , aeration flow rate: 400 mL min ⁻¹ , initial dye pH: ~6.5, light source: 45 watts compact fluorescent lamp	94
Figure 3.27	Photodegradation experiment of RR4 dye under visible light irradiation. Experimental conditions; dye concentration: 30 ppm, catalyst loading: 1.3 gL ⁻¹ , aeration flow rate: 400 mL min ⁻¹ , initial dye pH: ~6.5, light source: 45 watts compact fluorescent lamp equipped with UV filter	96
Figures 3.28	Photodegradation experiment of RR4 dye under solar irradiation. Experimental conditions; dye concentration: 30 ppm, catalyst loading: 1.3 gL ⁻¹ ,	98

aeration flow rate: 400 mL min⁻¹, initial dye pH:
~6.5, light source: solar irradiation

- Figure 3.29 The influence of initial dye concentration on the photocatalytic activity of CTHA0.025/650 photocatalyst. Experimental conditions; catalyst loading: 1.3 gL⁻¹, aeration flow rate: 400 mL min⁻¹, initial dye pH: ~6.5, light source: 45 watts compact fluorescent lamp 100
- Figure 3.30 The influence of initial dye concentration on the photocatalytic activity of CTPC0.20/620 photocatalyst. Experimental conditions; catalyst loading: 1.3 gL⁻¹, aeration flow rate: 400 mL min⁻¹, initial dye pH: ~6.5, light source: 45 watts compact fluorescent lamp 101
- Figure 3.31 Plot of the actual concentration of the dye removed by CTHA0.025/650 photocatalyst. Experimental conditions; catalyst loading: 1.3 gL⁻¹, aeration flow rate: 400 mL min⁻¹, initial dye pH: ~6.5, light source: 45 watts compact fluorescent lamp 102
- Figure 3.32 Plot of the actual concentration of the dye removed by CTPC0.20/620 photocatalyst. Experimental conditions; catalyst loading: 1.3 gL⁻¹, aeration flow rate: 400 mL min⁻¹, initial dye pH: ~6.5, light source: 45 watts compact fluorescent lamp 103
- Figure 3.33 The influence of catalyst loading on the photocatalytic activity of CTHA0.025/650 106

	photocatalyst. Experimental conditions; dye concentration: 30 ppm, aeration flow rate: 400 mL min ⁻¹ , initial dye pH: ~6.5, light source: 45 watts compact fluorescent lamp	
Figure 3.34	The influence of catalyst loading on the photocatalytic activity of CTPC0.20/620 photocatalyst. Experimental conditions; dye concentration: 30 ppm, aeration flow rate: 400 mL min ⁻¹ , initial dye pH: ~6.5, light source: 45 watts compact fluorescent lamp	107
Figure 3.35	The effect of aeration flow rate on the photocatalytic activity of CTHA0.025/650 photocatalyst. Experimental conditions; dye concentration: 30 ppm, catalyst loading: 1.3 gL ⁻¹ , initial dye pH: ~6.5, light source: 45 watts compact fluorescent lamp	110
Figure 3.36	The effect of aeration flow rate on the photocatalytic activity of CTPC0.20/620 photocatalyst. Experimental conditions; dye concentration: 30 ppm, catalyst loading: 1.3 gL ⁻¹ , initial dye pH: ~6.5, light source: 45 watts compact fluorescent lamp	111
Figure 3.37	The influence of initial pH of the dye solution on the photocatalytic activity of CTHA0.025/650 photocatalyst. Experimental conditions; dye concentration: 30 ppm, catalyst loading: 1.3 gL ⁻¹ , aeration flow rate: 400 mL min ⁻¹ , light source: 45 watts compact fluorescent lamp	114

Figure 3.38	The influence of initial pH of the dye solution on the photocatalytic activity of CTPC0.20/620 photocatalyst. Experimental conditions; dye concentration: 30 ppm, catalyst loading: 1.3 gL ⁻¹ , aeration flow rate: 400 mL min ⁻¹ , light source: 45 watts compact fluorescent lamp	115
Figure 3.39	COD disappearance as the function of irradiation time. Experimental conditions; dye concentration: 60 ppm, catalyst loading: 1.3 gL ⁻¹ , aeration flow rate: 400 mL min ⁻¹ , initial dye pH: ~6.5, light source: 45 watts compact fluorescent lamp	118
Figure 3.40	COD disappearance as the function of irradiation time. Experimental conditions; dye concentration: 60 ppm, catalyst loading: 1.3 gL ⁻¹ , aeration flow rate: 400 mL min ⁻¹ , initial dye pH: ~6.5, light source: solar irradiation	121
Figure 3.41	Relative concentration of phenol as a function of irradiation time	124
Figure 3.42	COD disappearance as the function of irradiation time. Experimental conditions; phenol concentration: 10 ppm, catalyst loading: 1.0 gL ⁻¹ , aeration flow rate: 400 mL min ⁻¹ , light source: 45 watts compact fluorescent light	125
Figure 3.43	Changes in relative concentration of RR4 with cycling operations of photodegradation using CTHA0.025/650 and CTPC0.20/620 photocatalysts	126

LIST OF ABBREVIATIONS

C	Carbon
HA	Humic acid
PC	Peat coagulant
THA	Humic acid dopedTiO ₂
TPC	Peat coagulant doped TiO ₂
CTHA	Carbon doped TiO ₂ from humic acid precursor
CTPC	Carbon doped TiO ₂ from peat coagulant precursor
RR4	Cibacron brilliant red
ppm	Part per million
UV	Ultraviolet
COD	Chemical oxygen demand
CdS	Cadmium sulfide
PL	Photoluminescence
XRD	X-ray diffraction
CHN	Carbon, Hydrogen, Nitrogen
SEM	Scanning electron microscope
EDX	Energy dispersive X-ray
FTIR	Fourier transform infra red
HTT	Heat treatment temperature

**PENYEDIAAN DAN PENCIRIAN TiO₂ TERDOP KARBON
MENGUNAKAN ASID HUMIK DAN TERBITAN TERUBAHSUAINYA
SEBAGAI PREKURSOR KARBON UNTUK PENINGKATAN AKTIVITI
FOTOPEMANGKINAN.**

ABSTRAK

TiO₂, suatu fotomangkin semikonduktor yang mesra alam dan ekonomi menjadi tumpuan kajian saintifik yang pesat sejak 10 tahun yang lalu. Walau bagaimanapun, TiO₂ hanya mampu diaktifkan oleh cahaya UV disebabkan tenaga pengaktifannya yang besar iaitu 3.2 eV. Salah satu kaedah untuk meningkatkan aktiviti fotopemangkin TiO₂ adalah dengan cara mendopkan atom asing kedalam TiO₂, contohnya unsur-unsur bukan logam seperti N, C dan S. Dalam penyelidikan ini, TiO₂ terdop karbon telah disediakan dengan menggunakan dua jenis prekursor karbon iaitu asid humik (HA) dan terbitan terubahsuainya, penggumpal tanah gambut (PC). Proses penyediaan TiO₂ terdop karbon daripada asid humik (CTHA) dan penggumpal tanah gambut (CTPC) melibatkan dua peringkat utama iaitu proses mendop dan rawatan pemanasan. Nilai optimum bagi peratus pendopan HA dan PC ke dalam TiO₂ adalah 0.025 % dan 0.20 % masing - masing. Suhu optimum rawatan pemanasan untuk penyediaan fotomangkin telah dikenalpasti pada 650°C bagi CTHA dan 620°C bagi CTPC. Sampel yang disediakan seterusnya dicirikan melalui SEM-EDX, XRD, BET, CHN, spektroskopi UV-vis, FTIR dan spektroskopi fotopendarcahaya. Penilaian tahap fotopemangkin bagi sampel yang disediakan dijalankan dengan memantau eksperimen penguraian suatu pencelup anionik reaktif merah 4 (RR4) menggunakan sumber cahaya daripada lampu pendafluor cahaya

nampak 45 Watt dan juga cahaya solar. Pemalar kadar tertib pertama (k) bagi penguraian RR4 menggunakan sampel CTHA dan CTPC yang disinari lampu pendafluor cahaya Nampak 45 Watt ialah 0.041 dan 0.043 min^{-1} masing-masing. Nilai k untuk penguraian RR4 menggunakan TiO_2 terdop karbon adalah empat kali lebih cepat berbanding menggunakan TiO_2 tak di ubahsuai sebagai mangkin tindak balas. Manakala, bagi eksperimen di bawah cahaya solar, aktiviti fotopemangkinan didapati lebih tinggi iaitu dengan nilai k 0.168 dan 0.191 min^{-1} masing-masing menggunakan sampel CTHA dan CTPC. Peningkatan kadar pemfotomangkinan yang ditunjukkan oleh TiO_2 terdop karbon adalah disebabkan kandungan karbon di dalam fotomangkin ini yang bertindak sebagai penangkap elektron yang seterusnya mencegah gabungan semula pembawa-pembawa cas bebas. Kesan-kesan parameter pengoperasian yang diaplikasikan pada sistem seperti kepekatan pencelup RR4, muatan fotomangkin, kadar pengudaraan dan juga pH bagi larutan tindak balas telah di kaji. Keputusan menunjukkan bahawa penggunaan fotomangkin yang efisien dan pemilihan parameter pengoperasian yang optima akan membawa kepada mineralisasi lengkap bahan pencemar.

**PREPARATION AND CHARACTERIZATION OF CARBON DOPED TiO₂
USING HUMIC ACID AND ITS MODIFIED DERIVATIVE AS CARBON
PRECURSORS FOR ENHANCED PHOTOCATALYTIC ACTIVITIES.**

ABSTRACT

TiO₂, one of the semiconductor photocatalysts with environmental friendly and economical characteristics had attracted scientific interest over the last 10 years. However, TiO₂ can only be activated by UV light corresponding to its large band gap of 3.2 eV. One of the possible approaches in improving the photocatalytic activity of TiO₂ was via doping of foreign atoms such as non-metallic elements like N, C and S. In this study, carbon doped TiO₂ was prepared by using humic acid (HA) and its modified derivative, peat coagulant (PC) respectively, as the carbon precursors. The preparation process of the carbon doped TiO₂ (CTHA) from HA and carbon doped TiO₂ (CTPC) from PC photocatalysts involves two core stages that are doping and thermal treatment process. The optimum doping percentage was found to be 0.025 % and 0.20 % for the photocatalyst prepared from HA and PC respectively. The optimum treatment temperature for the preparation of the photocatalysts was identified at 650°C for CTHA and 620°C for CTPC photocatalyst. The prepared samples were characterized via SEM-EDX, XRD, BET, CHN, UV-vis, FTIR and photoluminescence analyses. The photocatalytic evaluation of the samples was carried out via photodegradation of an anionic dye, reactive red 4 (RR4) in aqueous suspension under illumination of 45 Watt visible light fluorescent lamp as well as under solar irradiation. First order rate constants (*k*) for the photodegradation of RR4 with CTHA and CTPC samples under 45 Watt visible light fluorescent lamp

irradiation was *ca.* 0.041 and 0.043 min⁻¹ respectively, which is about four times faster than the unmodified TiO₂. On the other hand, similar experiment performed under solar irradiation yielded higher photocatalytic activity with *k* value *ca.* 0.168 and 0.191 min⁻¹ respectively using CTHA and CTPC samples. The higher photocatalytic activity exhibited by carbon doped TiO₂ samples was attributed to the electron scavenging ability of the carbon particles contained in TiO₂. The effect of operational parameters such as dye concentration, catalyst loading, aeration rate as well as the pH of the solution has been examined. Results showed that the employment of efficient photocatalysts and the selection of optimal operational parameters may lead to complete mineralization of the model pollutant.

CHAPTER 1: INTRODUCTION AND LITERATURE REVIEW

1.1 General

The control of water pollution has become an increasingly important issue in recent years. The widespread disposal of industrial wastewater onto land and water bodies has led to serious contamination in many countries worldwide. Of all the pollution contributors, textile wastewater is classified as the most polluting among all industrial sectors in terms of both volume and composition of effluent[1]. Estimates indicate that approximately 15 % of the synthetic textile dyes produced worldwide are lost in wastewater streams during manufacturing or processing operations [2]. The removal rate of the textile dyes are low and thus they are considered as hazardous material wherein they would possibly form aromatic amines which are potentially harmful to the living world [3]. These dyes could also cause eutrophication in the water bodies along with severe reduction in water qualities [4].

The toxicity and mass production of the textile dyes emerged as the major focus of the environmental remediation efforts. There were several studies done on the physical, chemical and biological treatment of the dye containing effluents [5, 6]. Physical methods such as flocculation, reverse osmosis, membrane filtration and adsorption on activated charcoal are non-destructive and merely transfer the pollutant to other media, thus causing secondary pollution [5, 7-9].

Chemical methods are not practical economically due to the requirement of high dosage and production of large amount of sludges [10, 11]. Bio-treatment of azo dyes is ineffective due to their resistance to aerobic bio-degradation. Besides, anaerobic bio-degradation of azo dyes may generate carcinogenic aromatic amines

[12-14]. There is thus an urgent need for the textile industries to develop a new effective method for their wastewater processing.

In the last two decades, efforts have been devoted to the study of photochemical process in heterogeneous systems. In view of this, photocatalytic degradation of contaminants using semiconductor seems to be a very promising way for the treatment of wastewater from the textile industries. The so-called photocatalytic technique provides a more effective approach in wastewater treatment as compared to other conventional methods because semiconductors are inexpensive and it's capable of removing various organic and inorganic compounds.

1.2 Semiconductor Photocatalysts

The recent years has seen the embryonic scenario on the utilization of semiconductors as the photocatalyst to degrade various organic and inorganic pollutants in wastewater. Since the pollutant could be completely degraded into harmless materials by photocatalysis technique under normal temperature and air pressure, it has become a kind of water treatment technology with the best prospect of exploitation and utilization.

Photocatalysis technique through its photocatalytic degradation processes has proven to be a promising technology for the degrading various organic compounds such as phenols, colorants, surfactants, pesticides and cyanides [3, 15, 16] into harmless compounds like CO_2 and H_2O by irradiation with light. Compared with other conventional chemical oxidation methods, photocatalysis may be a more effective technique since the semiconductors are inexpensive and capable of mineralizing various refractory compounds [17].

Semiconductors can act as sensitizers for light-induced redox processes due to their electronic structure which is characterized by a filled valence band and an empty conduction band [18]. Various semiconductors other than TiO₂, such as ZnO, Fe₂O₃, CdS, ZnS, etc can be used as photocatalysts for the degradation of organic contaminants. Unlike metals which have a continuum electronic states, semiconductors possess a void energy region where no energy levels are available to promote recombination of an electron and hole produced by the photoactivation in their solid states. The void region is called the band gap which extends from the top of the filled valence band (VB) to the bottom of the vacant conduction band (CB) [19]. The valence band is located at energy level E_v and is fully occupied whereas the conduction band with higher energy E_c is empty [20]. The energy of the band gap E_g between these bands is equal to the difference between the conduction band and the valence band

$$E_g = E_c - E_v \quad (1.1)$$

The photocatalysis over semiconductors is initiated by the absorption of a photon with energy equal to or greater than the band gap of the semiconductor, producing electron-hole ($e^- - h^+$) pairs. The generation of electron-hole pairs and its reverse process could be represented by the following equations



where h is the Planck's constant ($h = 6.63 \times 10^{-34} \text{ Js}^{-1}$), ν is the frequency, e^- represents a conduction band electron, and h^+ represents a hole in the valence band. The electrons and holes produced from the excitation process could undergo subsequent

oxidation and reduction reactions with any species which might be absorbed on the surface of the semiconductor to give the final necessary products. The application of the illuminated semiconductors for the remediation of contaminants has been used successfully for a wide variety of compounds [3, 15, 16].

1.3 Basic Principles of Photocatalysis

In general, solids that can promote reactions in the presence of light and are not consumed in the overall reaction are referred to as “photocatalyst”. According to Mills and Hunte [21], the term “photocatalysis”, in its most simplistic description, is the “acceleration of a photoreaction by action of a catalyst”. “Photoreaction” here is defined as a “photoinduced” or “photoactivated” reaction, which both refers to the similar effect. In a heterogeneous photocatalysis system, photoinduced molecular transformation or reactions take place at the surface of the catalyst [19].

Photocatalytic reaction is initiated when light energy of a certain wavelength is made to fall on to a semiconductor. Absorption of the incident light with energy equivalent or exceeds the band gap energy of the semiconductor, generally leads to the photoexcitation of an electron from the valence band to the conduction band of the semiconductor particle, causing charge separation. The conduction band electrons and valence band holes can then migrate to the surface of the TiO₂ semiconductor and participate in the oxidation-reduction reactions [22]. The photocatalyst particles can act either as electron donors or acceptors for the molecules in the surrounding media. Figure 1.1 illustrates the excitation of an electron from the valence band to the conduction band initiated by the absorption of light. The excited electron and hole generated from the photoexcitation process could follow several possible

pathways. In aerated solution, the semiconductor at its surface can donate electrons to reduce an electron acceptor namely oxygen (pathway A). Sequentially, holes can migrate to the surface and combine with electrons from donor species (pathway B). The rate of the charge transfer processes depends on the redox potential of the adsorbent species as well as on the band-edge position of the band gap. The incidence of the recombination between electron and hole prohibits the migration of the charge carriers to the surface, thus impeding their reaction with the absorbed molecules [3]. Recombination can occur in the volume and at the surface of the semiconductor particle (pathway C and D, respectively) [19].

The efficiency and rate of a photocatalytic reaction particularly depends on the type of the photocatalyst and on the light radiation that is applied in its initiation process [20]. Additional aspects that influence a photocatalytic reaction are:

1. pH that affects the charge of a semiconductor surface,
2. concentration of the substrate that influence the reaction kinetics,
3. stream of photons, as oversupply of light accelerates the electron-hole recombination and
4. temperature, whereby higher temperature causes frequent collision between the semiconductor and the substrate.

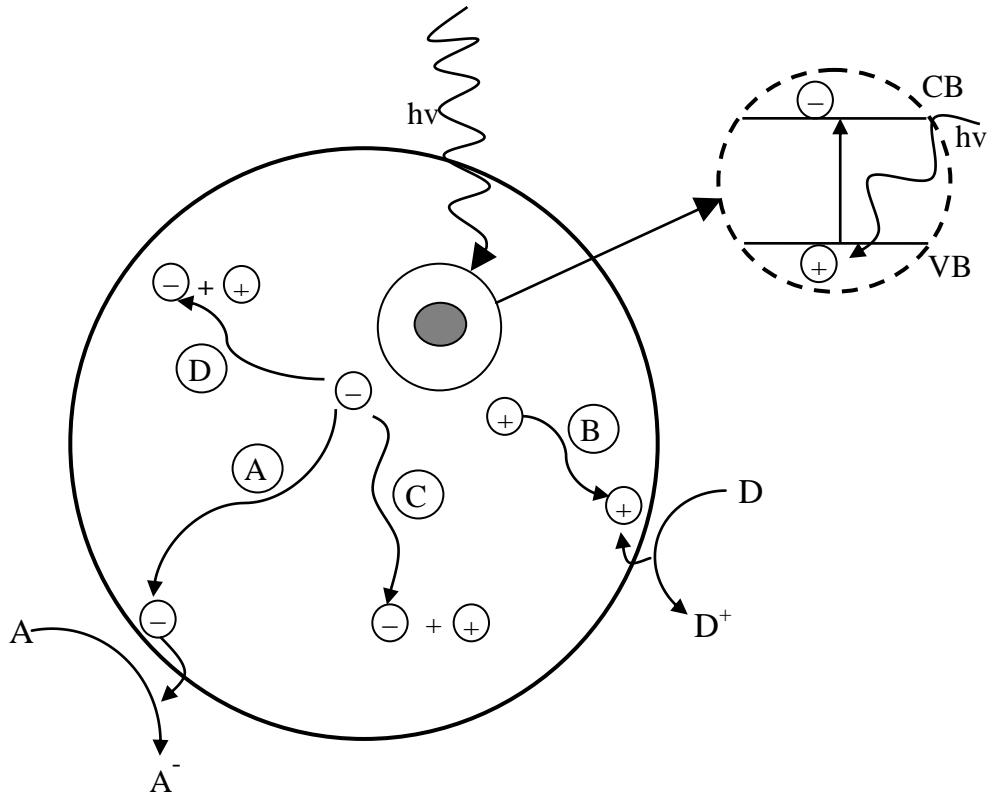


Figure 1.1: Schematic diagram on the general mechanism of TiO_2 photocatalyst [19].

1.4 Titanium Dioxide versus Existing Photocatalysts

Meisen and Shuai [20] have proposed the optimum characteristics necessary for a good photocatalyst. The features suggested are characterized by the following attributes:

1. The redox potential of the photogenerated valence-band hole must be positive enough for the hole to perform as an electron acceptor.
2. The redox potential of the photogenerated conduction-band electron must be negative enough for the electron to perform as a donor.
3. The material must not be prone to photocorrosion or produce toxic by-products.
4. The material should be commercially and economically available.

Chalcogenide semiconductors (oxides and sulfides) such as TiO₂, ZnO, Fe₂O₃, CdS, ZnS and WO₃ have been widely examined and used as photocatalysts for the decomposition of environmental organic contaminants [23]. However, not all of them are suitable for catalyzing oxidation and reduction reactions in the photocatalytic processes. The band gap energies of semiconductors commonly used for the photodecomposition of organic and inorganic compounds is presented in Table 1.1. The photoinduced transfer of electrons that take place with adsorbed species over the semiconductor photocatalyst depends on the band-edge position of the semiconductor and the redox potential of the adsorbates [24]. Metal sulfide semiconductors are unsuitable for the photocatalytic reactions due to their low stability as they readily undergo photoanodic corrosion. Even though the iron oxide polymorphs are inexpensive materials and exhibit nominally high band-gap energies, they are considered as unsuitable photocatalysts due to the fact that they easily suffer from photocatodic corrosion [20, 25].

Table 1.1: Band gap energies of selected semiconductors [23].

Photocatalyst	Bandgap energy (eV)	Photocatalyst	Bandgap energy (eV)
Si	1.1	ZnO	3.2
TiO ₂ (rutile)	3.0	TiO ₂ (anatase)	3.2
WO ₃	2.7	CdS	2.4
ZnS	3.7	SrTiO ₃	3.4
SnO ₂	3.5	WSe ₂	1.2
Fe ₂ O ₃	2.2	α-Fe ₂ O ₃	3.1

Among various oxide semiconductors used for the process of photocatalysis, titanium dioxide has essentially proved itself to be the most practical materials for widespread environmental applications mainly in water purification and wastewater treatment system. Titanium dioxide demonstrates many desirable properties as a good photocatalyst such as inexpensive, readily available material, more stable than other photocatalyst in ambient conditions and can be recycled. It is photoactive which enables it to utilize visible and/or near UV light and also non-toxic material. In addition, the corresponding photoelectrons have sufficient electronegativity to produce highly oxidizing radical species to affect the deep oxidation of a wide range of organic contaminants.

The positions of the redox potentials of various metallic couples related to the energy levels of the conduction and valence band of TiO_2 is presented in Figure 1.2. From the figure, it was pointed out that the redox potential of h^+ was found to be around +2.9. Therefore, any organic compound which has oxidation potential less than +2.9 supposedly will be oxidized. Since most of organic compounds have oxidation potential less than +2.9, theoretically the TiO_2 photocatalyst can be applied for the degradation of the organic pollutants in water.

Titanium dioxide exists in two common crystalline polymorphs i.e. anatase and rutile. The structure of the anatase and rutile forms can be described in term of chains of $(\text{TiO}_2)^{-6}$ octahedral. The two crystal structures differ by distortion of each octahedral and by the assembly pattern of the octahedral chains. Figure 1.3 shows the crystal structure of anatase and rutile. Anatase can be regarded to be built up from octahedrals that are connected by their vertices, whereas in rutile, the edges are connected [26]. These differences in lattice structure cause different mass densities

and electronic band structures between the two forms of titanium dioxide which leads to significant differences in many physical properties [3].

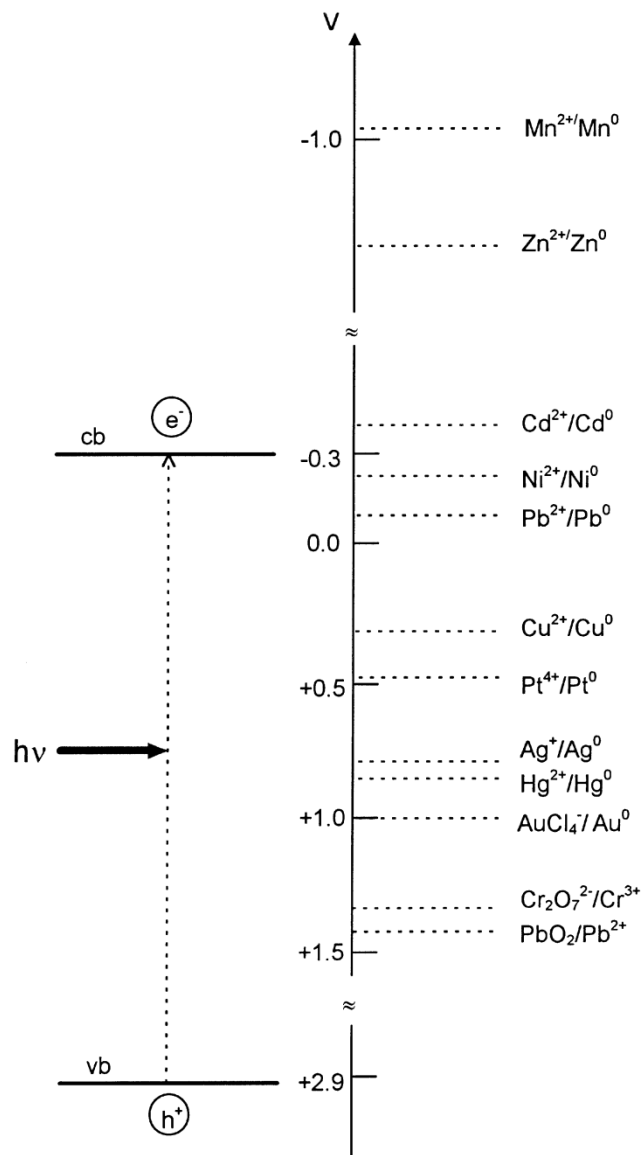


Figure 1.2: Positions of the redox potentials of various metallic couples related to the energy levels of the conduction and valence band of TiO_2 [27].

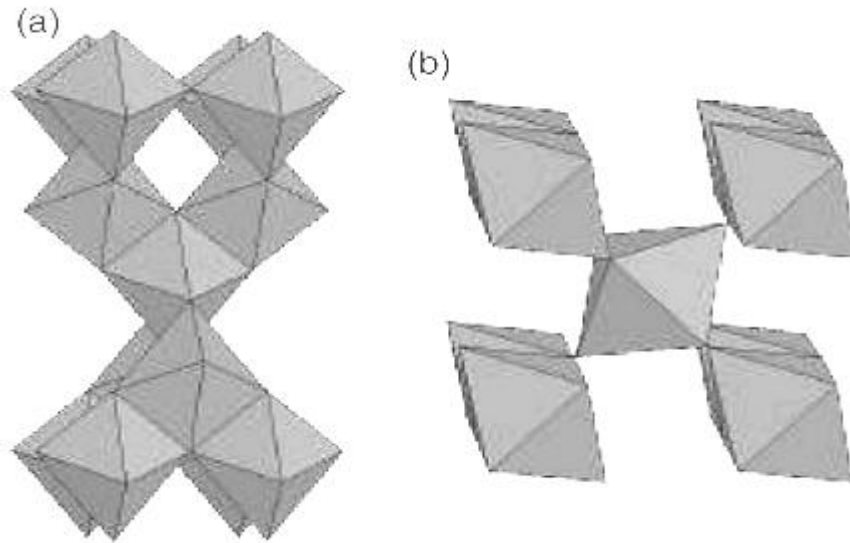


Figure 1.3:Crystal structure of (a) anatase and (b) rutile [26].

Both anatase and rutile are semiconductors with the band gap located at about 3.2 eV and 3.0 eV, respectively. Rutile does absorb some visible light, while anatase only absorbs in the UV region of spectra. Unfortunately, rutile is not a good photocatalyst [28]. Many researchers have concluded that rutile is catalytically inactive or a much less active form of TiO₂ [29, 30]. Anatase form of titanium dioxide therefore appears to be the most efficient semiconductor for environmental application. Its photocatalytic activity is higher than most other available crystalline forms of TiO₂. Based on the desirable properties revealed by the photocatalyst, researchers have devoted a few characteristic of TiO₂ photocatalyst that made it possible for utilization in a commercial scale water treatment system:

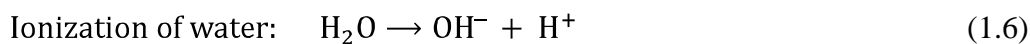
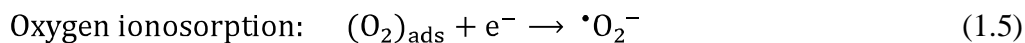
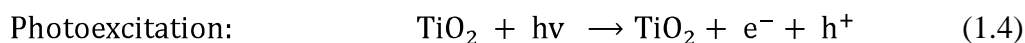
1. The reaction of photocatalysis takes place at room temperature [31].
2. Photocatalytic reactions do not suffer the drawbacks of photolysis reactions in terms of the production of intermediate products because organic pollutants are usually completely mineralized to non-toxic substances such as CO₂, HCl and water [32, 33].

3. The photocatalyst is inexpensive and can be supported on various substrates such as glass, fibers and stainless steel in order to allow for continuous re-use [31].
4. Photogenerated holes are highly oxidizing and photogenerated electrons reduce sufficiently to produce superoxides from the dioxygens [24].

1.5 General Mechanism of TiO₂-assisted Photocatalytic Degradation of Pollutants

The photocatalyst derives its activity from the fact that when photon of a certain wavelength are incident upon its surface, electrons are promoted from the filled valence band to the empty conduction band as the absorbed photon energy is equal or greater than the band gap energy of the photocatalyst. The excitation process will leave behind a positively charged hole in the valence band and accordingly an electron and hole pair (e^-h^+) is generated. The energized holes and electrons can either recombine and dissipate the absorbed energy as heat or be available for use in the redox reactions. The valence band hole and conduction band electron could react with electron donor or acceptor species absorbed on the TiO₂ surface [34]. In aerated aqueous suspension, the electrons can reduce absorbed oxygen to form superoxide radical ($\cdot O_2^-$) that can further disproportionate to form $\cdot OH$ through various pathways [35]. On the other hand, hydroxyl radicals which are strong oxidizing agents are formed from holes reacting with either H₂O or OH⁻ molecules adsorbed on the TiO₂ surface [36-38]. In addition, the band electrons may also react directly with contaminants via reductive processes [39]. Repeated attacks of the radicals on the pollutant species in the reacting system essentially leads to the complete mineralization of the organic molecules.

The following chain reactions have been widely postulated [3]:



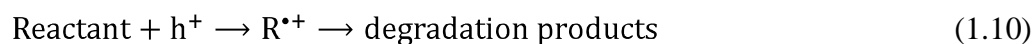
Formation of radicals by photo holes:



Oxidation of the organic reactant via successive attacks by $\cdot\text{OH}$ radicals:



or by direct reaction with holes:



The efficiency of the TiO_2 photocatalytic process however is retarded by the high rate of electron-hole pair recombination process. This becomes a formidable obstacle for realizing high efficiency in the photocatalytic processes and represents its major drawback. Therefore, any development of an efficient photocatalyst that is capable of degrading pollutants and preventing against these recombination processes is always recognized as an important contribution in this field.

1.6 Improving TiO₂ Photocatalytic Activity

TiO₂ has been regarded as an excellent semiconductor photocatalyst which provides unique opportunity for the remediation of the polluted environment. In order to increase the activity of the TiO₂ photocatalyst, various methods have been developed. To date, three approaches of TiO₂ modification system have been studied. These are (1) impeding recombination by increasing the charge separation for higher photocatalytic efficiency; (2) extending the wavelength range response of TiO₂ to the visible region and (3) altering the selectivity or yield of a particular product [19]. Several examples of these approaches of improving the photocatalytic activity of TiO₂ are summarized in the following sections below. The general mechanism for the selected systems is presented in Figure 1.4.

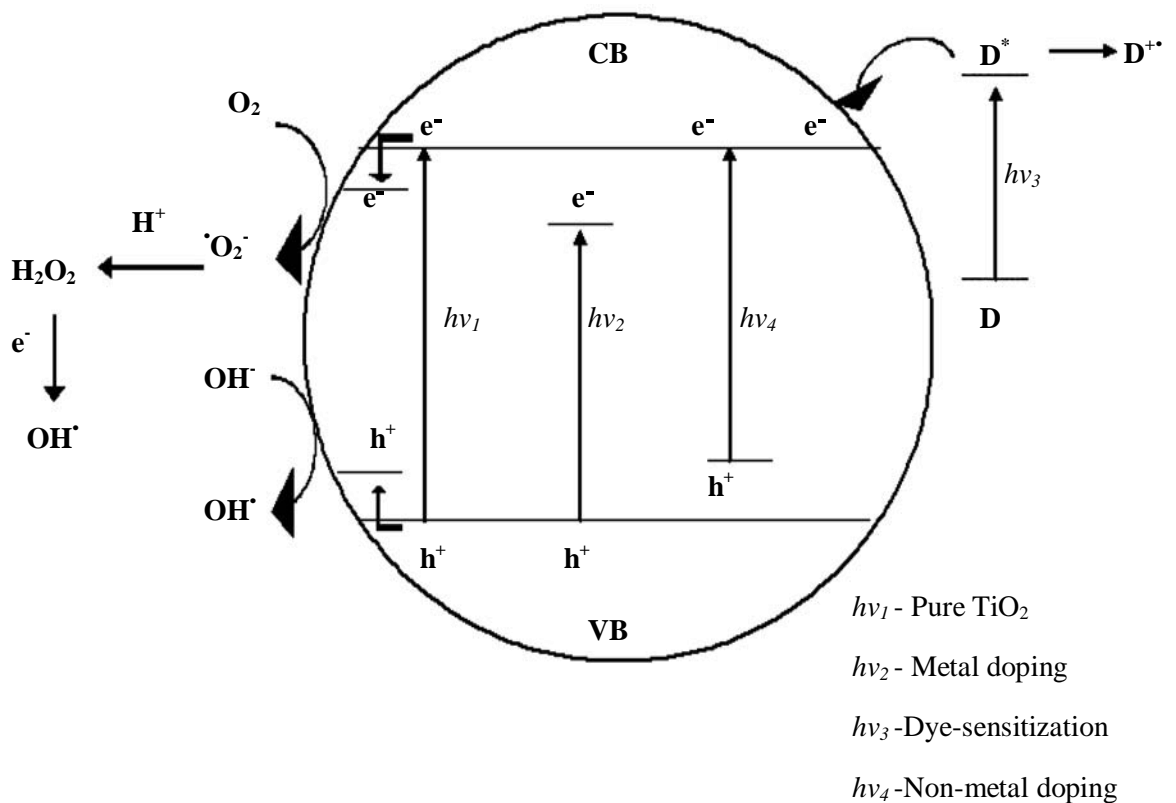


Figure 1.4: Several mechanism of modified TiO₂ photocatalysts [40].

1.6.1 Modification with metals

Addition of noble metals to a semiconductor can change the properties of the semiconductor surface thus could modify the pathway of the photocatalytic process. The metal can enhance the yield of the particular products or the rate of the photocatalytic reactions. Pt/TiO₂ system is one of the metal-semiconductor systems most commonly studied [41-43]. The addition of Pt to the TiO₂ surface is favorable for photocatalytic reaction evolving gas, mainly hydrogen [19]. The insertion of the noble metal actually modifies the photocatalytic properties of TiO₂ by changing the distribution of electrons which in turn affect the photocatalytic process on the semiconductor surface. The electronic modification of TiO₂ surface via metal deposition can also be observed with other noble metal such as Au [44, 45] and Ag [46, 47]. Besides photocatalytic enhancement, the modification through noble metals enables TiO₂ particles to be active in the energy range of the visible light [48]. However, the extensive utilization of noble metals for TiO₂ modification as a practical remediation technology is restricted because the noble metals are expensive.

Modification of TiO₂ with transition metals provides a successful and cost effective alternative as compared to the costly modification with noble metals. The addition of transition metals to TiO₂ was found to enhance the photocatalytic activity of the photocatalyst by UV irradiation and extend its application in the visible region of the electromagnetic spectrum. It was reported that the bombardment of TiO₂ semiconductor with metal ions from the transition series such as V, Cr, Mn, Ni and Fe brings about a red shift in the absorption pattern of the TiO₂ semiconducting catalyst. The order of the effectiveness in the red shift was found to be V>Cr>Mn>Fe>Ni [49]. The catalysts exhibited absorption in the range of 400-600 nm and thus could be effectively utilized under solar irradiation and work well in the

visible region of the spectrum. On the other hand, doping of TiO₂ with Fe³⁺ was affirmed to introduce much more oxygen vacancies in or on the crystals lattice and surface of TiO₂. This in turn would favour the adsorption of water and promote the formation of surface hydroxyl groups and hence enhanced the photocatalytic activity of the TiO₂. Beneficial effect of Fe³⁺ could also be elucidated by the efficient separation of the photoexcited electrons and holes. High concentration of dopant however increases the recombination rate and competed with the redox process and accordingly reduced the efficiency of the photocatalytic activity.

The studies on noble metals and transition metals modified TiO₂ revealed that there exists an optimum dopant concentration for the best photocatalytic performance of the modified TiO₂. The dosage level is an important factor in influencing the enhancement effect of the metals dopants. Below an optimum dosage level, the metals dopants can improve the charge separation by acting as electron-hole separation centre thus enhance the photocatalytic activity of the modified TiO₂. However, as dosage levels exceed optimum loading, they can act as electron-hole recombination centers which are detrimental to the photocatalytic activity [48, 50].

1.6.2 Modification with nonmetals

The widespread utilization of TiO₂ for the environmental remediation is to some extent constrained by its wide band gap (3.2 eV) energy, which requires ultraviolet irradiation for the photocatalytic activation. Since UV light accounts for only a small fraction (5%) of the sun's energy compared to visible light (45%), the shift in the optical response of TiO₂ from the UV to the visible spectral range will have a profound positive effect on the practical applications of the material [51].

Therefore, the most important and challenging issue is to develop efficient visible light sensitive photocatalyst by the modification of TiO₂. Doping TiO₂ with metal elements such as Fe, Cr, Co, Mo and V have been employed to tune the electronic structure and enhanced the photocatalytic activity of TiO₂ [49, 52]. However, metal doping exhibited several drawbacks: thermal instability of doped TiO₂, electron trapping by the metal centers, and requirement of more expensive ion-implantation facilities [53, 54]. Recently, many efforts have been made to modify titanium dioxide with nonmetals to efficiently extend the photoresponse from the UV to visible light region. The most important advances in the field are the development of visible light responsive TiO₂ photocatalyst doped with nonmetallic elements like N, C and S. Such modified TiO₂ materials exhibited larger absorption in the visible region and enhanced the degradation of organic dyes under visible light irradiation.

In order to obtain more insight of the issue concerning visible light response of the N-doped TiO₂, Asahi et al [51] had calculated the band structure of the N-doped TiO₂ for powder and thin film. They had proposed that oxygen sites in N-doped TiO₂ were substituted by nitrogen atoms subsequently contributes to the band gap narrowing. The relevant mechanisms for the role of nitrogen in N-doped TiO₂ are summarized as follows: The visible light absorption by N-doped TiO₂ is due to the substitution of oxygen by nitrogen in the TiO₂ lattice. The corresponding N (2p) states are located above the valence band edge. Mixing of N (2p) states with O (2p) states results in a reduction of the band gap of the N-doped TiO₂ thus increase the possibility for the photocatalysts to be utilized under visible light irradiation [51, 55].

Reports on band gap narrowing of TiO₂ by sulfur doping are also available in the literature. Periyat et al. [56] have reported about the preparation of high-temperature stable anatase titania with high photocatalytic activity by the

modification of titanium isopropoxide precursor with sulfuric acid. The high photocatalytic activity demonstrated by the samples can be explained by the high stability of the anatase phase due to sulfur doping, which leads to three main improvements in the modified sample namely increased surface area, band gap alteration and reduction in the crystallite size. The modification method also was able to eliminate the formation of various secondary and impure phases such as metal titanates and/or metal oxides at high temperature, which can lead to the reduction of the photocatalytic activity of the photocatalyst [56]. Another work by Umebayashi et al. [57] suggested that sulfur could be doped as an anion and replaced the lattice oxygen in TiO₂. They revealed that S-doping shifted the absorption edge of TiO₂ to a lower energy and demonstrated its photocatalytic activity via the photocatalytic degradation of methylene blue under visible light irradiation.

Doping with carbon atoms has attracted much attention in the last decade. It was reported that carbon could improve the activity of TiO₂, stabilize anatase structure and increase absorption of organic molecules on the catalyst surface [58-60]. For composites of photocatalyst TiO₂ and carbon, three possibilities have been reported namely TiO₂-mounted activated carbon, carbon doped TiO₂ and carbon coated TiO₂.

TiO₂-mounted activated carbon has been studied and some success was obtained for the coupling of the photocatalytic activity of anatase-type TiO₂ with the adsorptivity of activated carbon (AC) [58, 61-64]. Enhanced photocatalytic performance of TiO₂/AC composites was explained by the high adsorption of the impurities on the surface of the activated carbon and their transfer to TiO₂ surface. TiO₂/AC composite had been prepared by Tryba et al. [63], and it was noted that such photocatalyst was successfully used for the decomposition of phenol in water

while another study carried out by Nagaoka et al. [65] demonstrated the effective utilization of carbon/TiO₂ for decomposition of acetyldehyde. TiO₂/AC composite was recognized to exhibit several benefits such as improving the crystalline structure of the TiO₂ photocatalyst by using higher temperature of heat treatment and selection of proper carbon precursor for the carbonization. The carbon adsorbent should have high adsorption capacity for the targeted substances and the diffusion of the adsorbed substrates should not be seriously hindered [66].

Carbon-coated TiO₂ photocatalyst have been prepared by the calcination of the powder mixture of TiO₂ photocatalyst with the different carbon precursors such as poly (vinyl alcohol) (PVA), poly (ethylene terephthalate) (PET), or poly (vinyl chloride) (PVC) at high temperature from 500 to 1100 °C in inert atmosphere [58, 67-70], and pyrolysis of the highly dispersed sucrose on the surface of titania in flowing N₂ [71]. Carbon coating of titanium dioxide photocatalyst had several advantages, such as high adsorptivity and the suppression of the phase transformation from anatase to rutile, which usually occurs during the heating of the TiO₂ at 700 °C. This process improved the crystallinity of the anatase phase in TiO₂, which is responsible for its high photoactivity. Nevertheless, some drawbacks of the method also had been reported, such as the reduction in the amount of UV rays reaching the surface of TiO₂ particles caused by the carbon coating [72]. Therefore, the most important part is to get the balance among these factors in order to achieve a high performance of the photocatalyst.

Carbon doped TiO₂ could be attained by the mild oxidation of titanium carbide (TiC) in air at 350 °C [73], calcinations of TiO₂ with the mixture of urea and thiourea [74] or the oxidation of TiC at high temperatures [75]. It had been recognized for its various advantageous that affect the visible light activity of TiO₂

such as the narrowing of the band gap, the visible light absorption, and the transfer of the photoexcited carriers to the reactive sites at the catalyst surface [73, 76]. The carbon doped TiO₂ was different from carbon-coated TiO₂ in term of carbon content and color. The carbon doped anatase contained less than 1 wt % carbon and was yellowish, but carbon-coated anatase contained more than 2 % carbon and of a black color [70]. Choi et al. [75] have investigated the carbon doped TiO₂ and claimed that the substitution of C for O in the TiO₂ leads to a photocatalytic decomposition of methylene blue under visible light irradiation. Another study by Di Valentin et al. [77] revealed that the carbon doping of the TiO₂ favors the formation of oxygen vacancy which could be responsible for the extension of its photocatalytic activity to the visible range.

1.6.3 Modification with CdS: Composite semiconductors

The major drawback that confines the application of TiO₂ photocatalyst in the degradation of organic pollutant in water is the high rate of the recombination of the photogenerated electron-holes pairs. This phenomenon results in the poor rate of electrons and holes reaching the interface between semiconductor and water where the degradation is inherent to take place. The problem can be overcome by coupling a large band gap semiconductor with a smaller band gap semiconductor with suitable potential energies [19, 26]. To this end, CdS which have narrower band gap was reported to be an ideal sensitizer for the modification of TiO₂ [26, 78]. The coupling of the two semiconductor photocatalysts provides an interesting way to increase the efficiency of a photocatalytic process by enhancing the charge separation and increasing the lifetime of the charge carriers. Under visible light irradiation, the

energy of the excitation light is large enough to excite an electron from the valence band across the band gap of CdS ($E_g = 2.5$ eV) to the conduction band of TiO₂. The photogenerated electrons produced from the excitation process in CdS are transferred into the TiO₂ particles while the holes remained in the CdS particles. The electron transfer from CdS to TiO₂ increases the charge separation and efficiency of the photocatalytic process. Yu et al. [78] developed a microemulsion-mediated solvothermal method and prepared nanocrystalline TiO₂ coupled by highly dispersed CdS nanocrystals. This method can avoid the oxidation of CdS in the CdS-TiO₂ nanocomposites during the post-thermal treatment for the crystallization of TiO₂. The experimental result suggested an effective transfer of photogenerated electrons from the conduction band of CdS to that of TiO₂, leading to the minimization of the electron-hole recombination and longer charge separation. CdS-TiO₂ couples have also been prepared through a sol-gel method by precipitating TiO₂ on CdS [79]. These CdS-TiO₂ couples were found to exhibit a fast degradation rate, which were twice that of pure CdS and at least five times that of TiO₂. The coupled system extends the photoresponse of the photocatalyst into the visible range which makes it feasible for the organic dyes degradation under visible light illumination. However, one major drawback of utilizing CdS in the coupled system is that a significant quantities of toxic cadmium could be released into the aqueous media from the photoanodic corrosion of CdS-based system [79].

1.6.4 Dye-sensitized titanium dioxide photocatalyst

Another innovative approach in improving photocatalytic activity of TiO₂ is via dye sensitization technique. In this system, a sensitizer which is usually selected

from colored compounds is anchored onto the surface of TiO₂. There are several ways of anchoring the sensitizer onto the surface of TiO₂ particles as reported by Kalyanasundaram et al. [80] such as through covalent bonding, ion-pair type association, physisorption, entrapment in cavities or pores and hydrophobic interactions leading to self-assembly of monolayers.

Significant work has been reported in the field of degradation of textile dyes into harmless end products under visible light irradiation [81-83]. Reports on the degradation of dyes like the methylene blue, Remazol Brill Blue R (RBBR) and orange G (OG) via dye sensitized TiO₂ system had also been available in the literature [84]. Basically, the mechanism involves 1) the adsorption of the dye on to the surface of TiO₂, 2) charge injection from the excited dye molecule into the conduction band of TiO₂ under visible light irradiation, 3) reaction of migrated electron with oxygen molecule at the surface of TiO₂ forming superoxide radical anion and 4) successive attacks of the radical on the dye molecule to convert it to non-toxic harmless end products.

Dye sensitization technique has also been noticed to be workable for colorless pollutant in wastewater. Several researchers have reported about the degradation of phenols and its derivatives using the method of dye sensitized TiO₂ [85, 86]. The degradation of other organic pollutant such as halocarbons, surfactants and pesticides by the dye modified TiO₂ had also been reported [87-89]. The result of those studies indicated that the presence of sensitizers was beneficial for the photoactivity of the TiO₂. The possible advantages of dye sensitized TiO₂ system was summarized as follows [3]:

1. Extends the range of excitation energies of TiO₂ into visible region.

2. Increase the sensitivity of the photocatalytic process for the removal of colored pollutants (in systems with low concentration of colored pollutants).

However, the dye sensitization of TiO₂ system had encountered a few difficulties that limit its performance as an environmental purifier, for example the reduction of the injection efficiency due to internal filtering caused by the adsorption of additional dye layers on the semiconductor, poor overlapping of the sensitizer adsorption with solar emission spectrum and weak coupling of electronically excited dye molecule with acceptor states of the semiconductor substrate [3].

1.7 Potential Natural Products for TiO₂ Sensitizers and Carbon Precursors

1.7.1 Humic acid

Humic acid (HA) is a major fraction of humic substances composed of a long chain molecule. It is a naturally occurring polymer which is high in molecular weight, dark brown in color and soluble in an alkaline solution. Humic acid can be found in peat, coal, many upland streams and ocean water. They are known to be high in carbon content (50-60%) of both aliphatic and aromatic character and rich in oxygen containing functionalities such as carboxyl, phenolic, alcoholic, and quinoid groups [90].

Humic acid account for an imperative fraction of natural organic carbons in surface waters and soils and play many important roles as a photosensitizer in aquatic photochemical processes, a complexing agent for heavy metal ions, and an organic coating material on mineral surfaces [90]. Upon electronic excitation, humic acid produced reactive species that act as depolluting agents in the natural waters by

photoinducing the degradation of organic pollutants [91]. Accordingly, humic acid have received much attention in relation to water treatment and its role as the photosensitizers or photoinitiators in the degradation of pollutants in water [90, 92, 93].

1.7.2 Peat coagulant

Peat soil is a natural inexpensive material rich in humic substances. It is a light brown to black organic sediment formed under waterlogged conditions from the partial decomposition of mosses and other bryophytes, sedges, grasses, shrubs or trees [94]. In Malaysia, peat has been identified as one of the major groups of soils where approximately 3.0 millions hectares of land area or 8% of the whole country is covered with peat soil. Malaysia peat soil is categorized as tropical peat soil and it is different both chemically and structurally from the peat soil found in Europe and Canada due to its exposure to the tropical climate. This peat is considered as a problem soil for vegetation because of their poor nutrient content and acidic nature [95].

In order to expand value-added products of tropical peat soils, peat coagulant was prepared using tropical peat soil of Malaysia [95, 96]. Peat coagulant is a chemically modified peat soil where a positively charge functional group was introduced. The characterization of the peat coagulant revealed that phenolic and carboxylic groups contained in the peat soil were utilized for the attachment of the ethylenediamine facilitating it to function as coagulant [94-96]. Preparation of the peat coagulant is a single and non-hazardous process where it only involves minimum requirement of chemicals and utilities. The low cost preparation methods

of peat coagulant highlighted its high potential to be manipulated as a cost effective technique for water treatment system. Having the advantage of wide pH working range, it was also reported to be effective coagulant for the clarification of lake water as well as the textile waste water [94-96].

1.8 Reactive Red 4 Dye

Azo dyes are abundant class of synthetic, colored, organic compounds which represent the largest class of dyes in use nowadays. It is characterized by the presence of one or more azo bonds ($-N=N-$) and it can be divided into monoazo, diazo and triazo classes according to the number of azo bonds available. According to this, reactive red 4 (RR4) or commonly known as cibacron brilliant red dye is classified as a monoazo dye as it possesses only one azo bond in its structure. Azo dyes and their dye precursors have been reported to be human carcinogenic as they could form toxic aromatic amines [3, 97]. These dyes may build up in the environment and pose a major threat to the surrounding ecosystem since many wastewater treatment plants allow these dyes to pass through the system virtually untreated. The increased public concerned with these documented health hazards and environmental pollutants have prompted the need to develop a treatment method for converting such colored effluents to harmless compounds. Indeed, the capability of TiO_2 photocatalyst in dealing with the destruction of these dyes has become a major reason of its growing application during the last decade. The structure of reactive red 4 dye is shown in Figure 1.5.

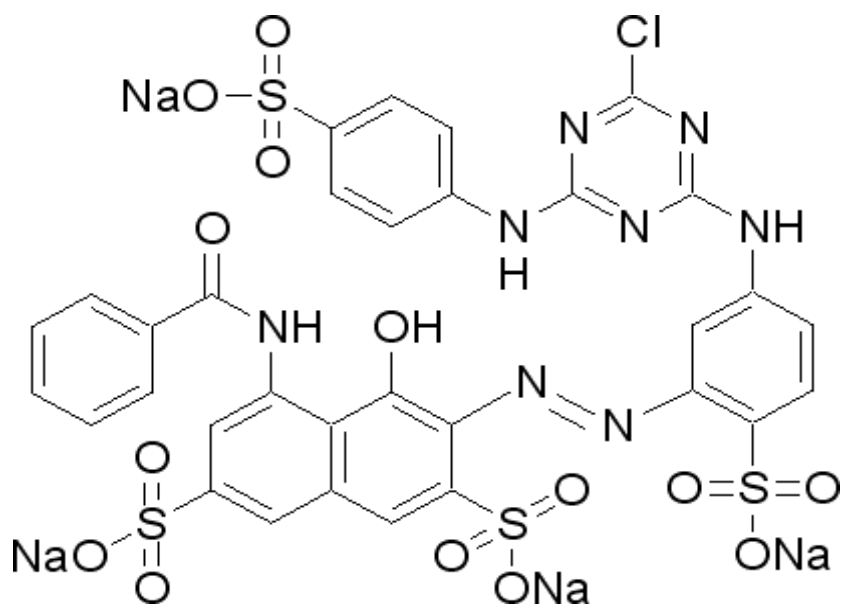


Figure 1.5: Molecular structure of RR4 dye.

1.9 Problems Statement

Up till now, numerous efforts have been made in developing carbon-TiO₂ composites as a clean technology for environmental remediation. However, there are still a few unsolved problems in this area that remains unexplored. Based on the literature study discussed earlier, a few problems have been identified:

1. Numerous work on the carbon-modified TiO₂ produced photocatalyst with high carbon content (> 1%) where the result was less effective than unmodified TiO₂.
2. Very few works implemented natural polymer as the carbon precursor. Most works utilized synthetic polymer such as polyvinyl alcohol (PVA) and polyethylene (PET).